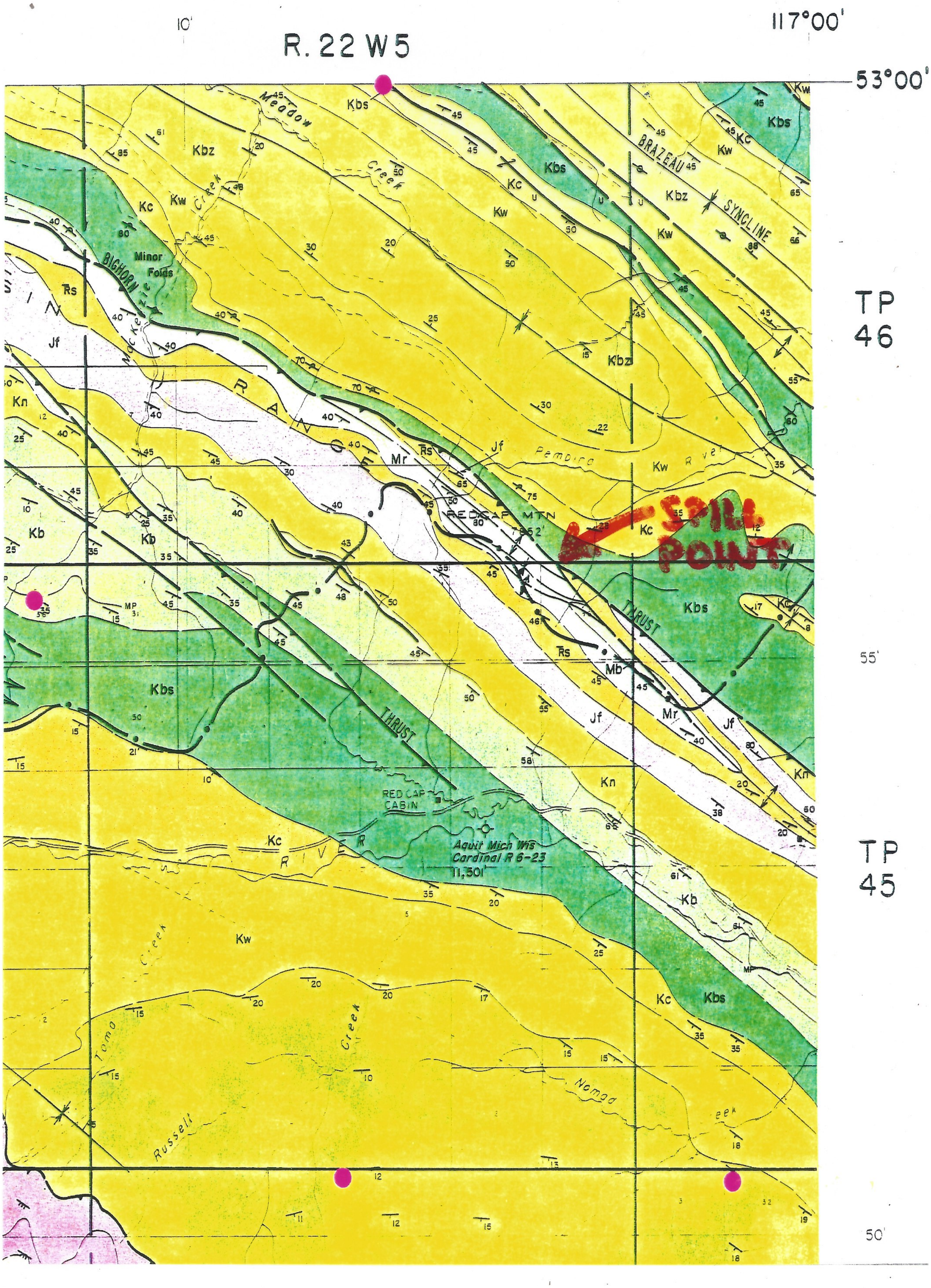
10'
R. 22 W5
117°00'
53°00'
TP 46
55'
TP 45
50'
SPILL POINT
Meadow Creek
Kbs
Kbz
Kc
Kw
BRAZEAU SYNCLINE
BIGHORN
Minor Folds
Mackenzie Creek
Rs
Jf
Kn
Kb
Mr
RANGE
REDCAP MTN
7852'
Pembina River
THRUST
Mb
MP
RED CAP CABIN
Aquit Mich Wis Cardinal R 6-23
11,501'
RIVER
Tomo Creek
Creek
Russell
Nomad Creek

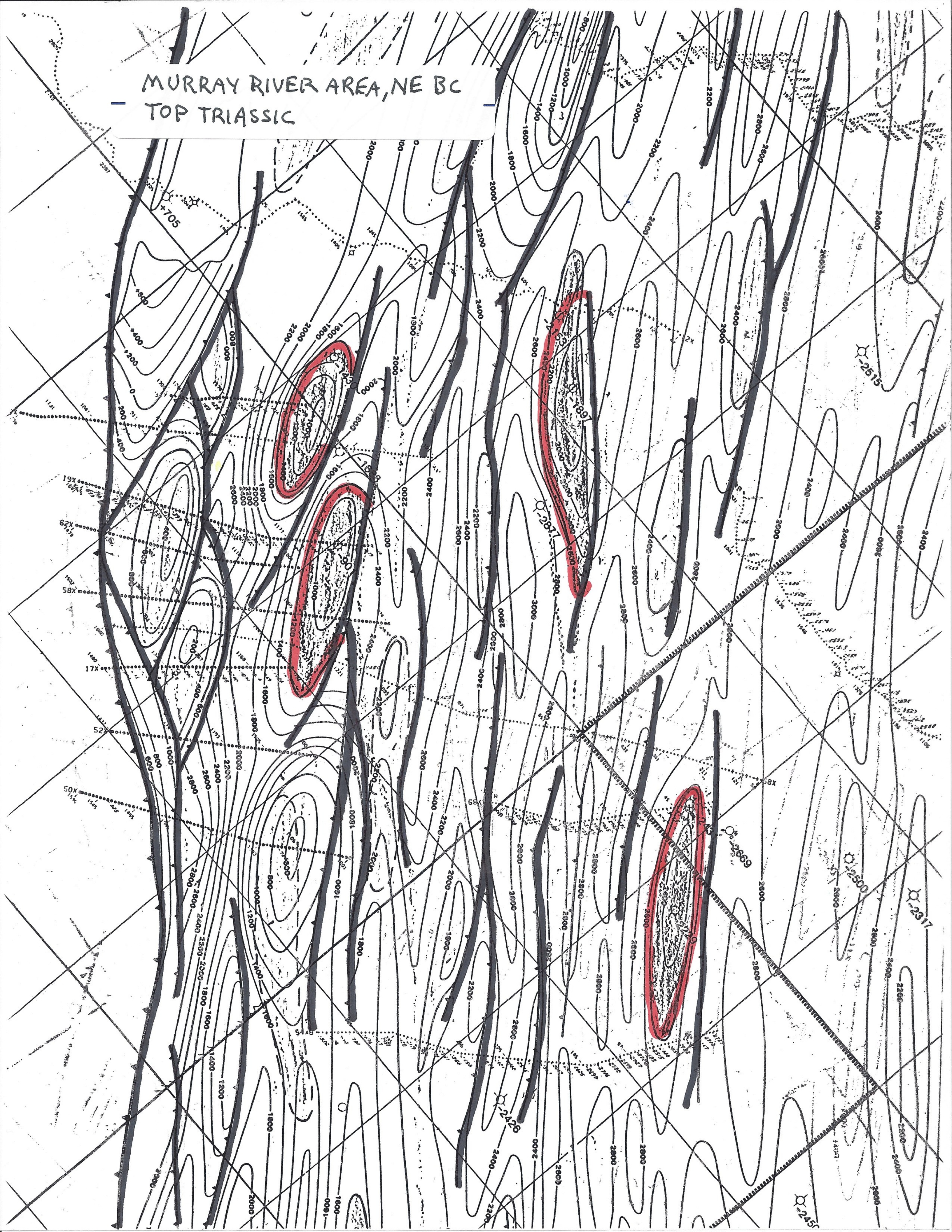
MURRAY RIVER AREA, NE BC
TOP TRIASSIC

THRUST FAULT LINKAGE

&

CONSIDERATIONS FOR TRAP INTEGRITY

Dave Klepacki
March 7, 1994

Thrust Fault Linkage and Considerations for Trap Integrity.

Dave Klepacki, PanCanadian Petroleum, Ltd., 900 125 9th Ave S.E., Calgary, Alberta, T2G-0P6

Large thrust faults typically comprise several "lower order" strands that have linked to form a single "first order" surface. For example, the McConnell Thrust comprises at least five such linked strands. The concept whereby fault strands propagating laterally capture one another to form a major fault was originally discussed by Douglas (1958) and sketched out by Jones (1971). Displacement fields along individual thrust strands are apparently sinusoidal (Ratliff, 1992) similar to the "bow and arrow" displacement generalization proposed by Elliot (1976). The displacement field of a major thrust is also broadly sinusoidal but has local maxima and minima, apparently related to the maxima and junctures (branch lines) of the original second order strands (Liu and Dixon, 1991). The local displacement maxima commonly correspond to structural culminations (hanging wall ramps or fault-propagation folds) along the thrust surface and are the principal hydrocarbon traps in the foothills belt. Examples are Quirk Creek, a local maximum along the Highwood sheet, and Castle River, a local maximum along the "Waterton sheet".

The geometry of fault juncture is important for hydrocarbon exploration. The tip of the "captured" fault may breach the top seal of a culmination forming along the "capturing" strand (which becomes the major thrust surface). Such breached seals account for some underfilled and uneconomic hydrocarbon traps. An understanding of the 3-D geometry and evolution of the fault network will increase our predictive skills and minimize any disappointments.

Douglas, R. J. W., 1958, Mount Head map-area, Alberta. Geological Survey of Canada Memoir 291, 241 p.
Elliot, D, 1976, The energy balance and deformation mechanisms of thrust sheets. Phil. Trans. R. Soc. London, A283: p 289-312.
Jones, P.B., 1971, Folded faults and sequence of thrusting in Alberta Foothills. AAPG Bulletin v.55, no.2, p. 292-306.
Liu, S., and Dixon, J.M., 1991, Centrifuge modelling of thrust faulting: structural variations along strike in fold-thrust belts. Tectonophysics, 188, p. 39-62.
Ratliff, R., 1992, Ph.D. Thesis, University of Colorado

Dave Klepacki: Fault Linkage & Trap Integrity Considerations

Outline:

- Fault linkage Geometry
  - 1) Jumping Pound
  - 2) Segments of McConnell Thrust
  - 3) Linkage near Brazeau River
- History
  - 4) Douglas
  - 5) Jones
- Displacement fields
  - 6) Elliot Diagram
  - 7) Turner Valley, Highwood Sheet
  - 8) Ratliff Displacement Profiles
  - 9) Displacement Equations
  - 10) Hinge lines Frannie Fold
  - 11) Linear-Arith Best Fit
  - 12) Liu (Multiple thrusts)
- The Model
  - 13) Two Faults propagating and linking
- Examples
  - 14) Quirk Creek
  - 15) Castle River Profile
  - 16) Castle River
  - 17) Turner Valley
- Geometry of Capture
  - 18) Out of Sequence Capture
- Fault Breach
  - 19) Bighorn Thrust breached anticline
  - 20) Fault Breach Vu-Graph
  - 21) Shoot First, ask Questions Later

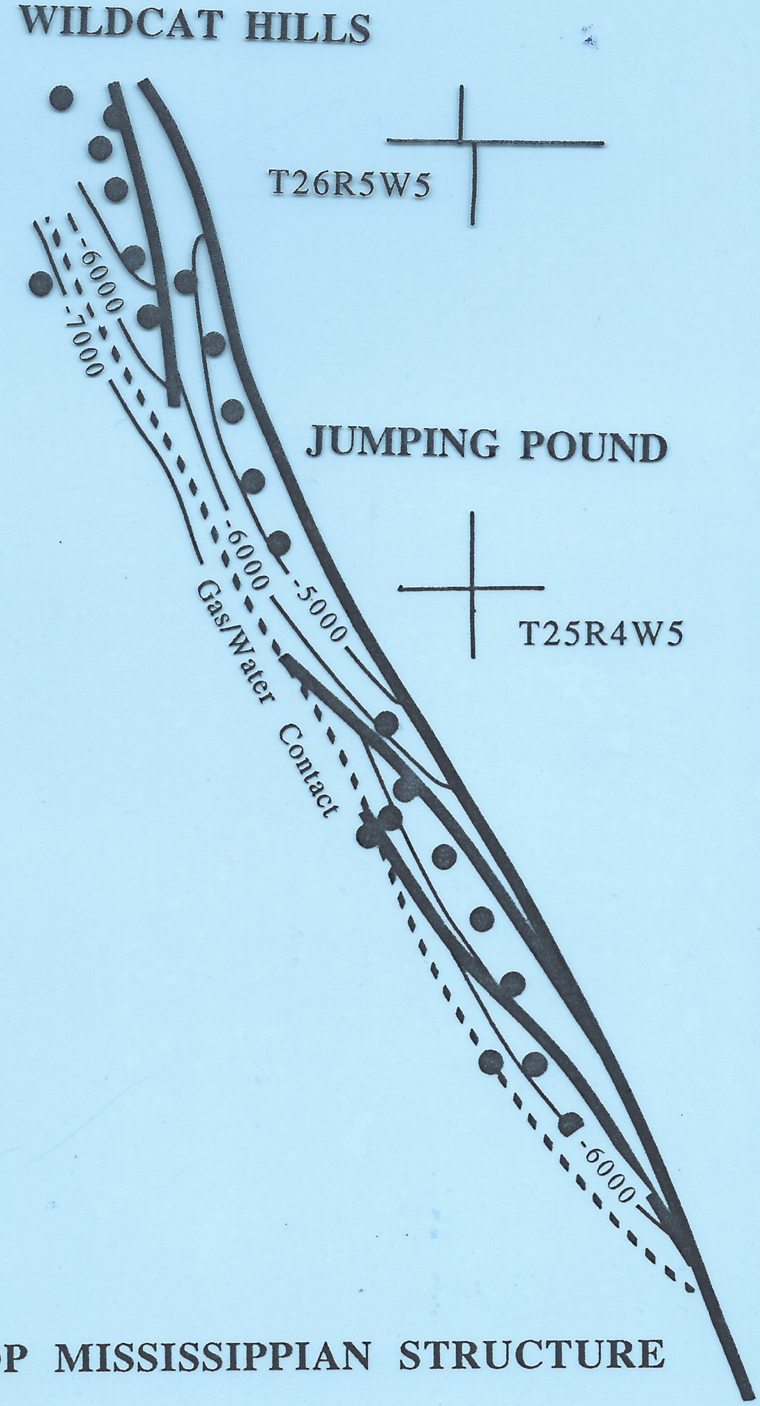

TOP MISSISSIPPIAN STRUCTURE

SEGMENTATION OF THE McCONNELL THRUST

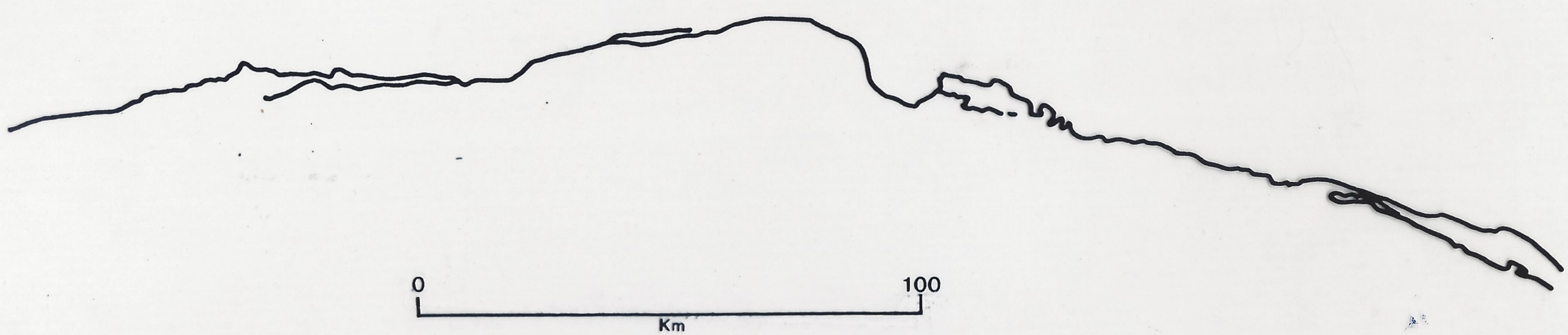

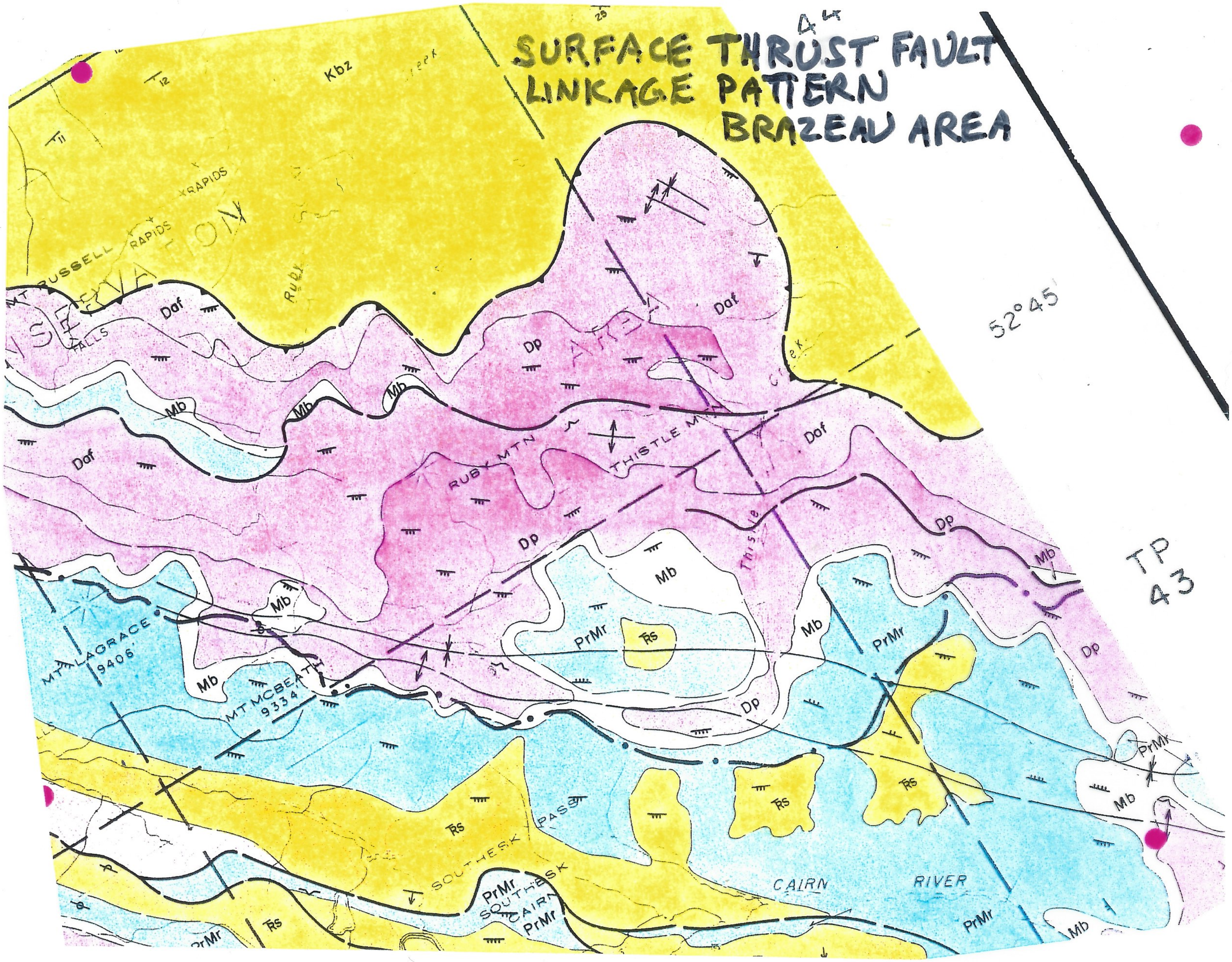

SURFACE THRUST FAULT
LINKAGE PATTERN
BRAZEAU AREA
44
52°45'
TP
43
Kbz
RAPIDS
RUSSELL
FALLS
Daf
Dp
Mb
RUBY MTN
THISTLE MTN
Thistle
PrMr
Rs
MT LAGRACE
9406
MT MCBEATH
9334
PASS
SOUTHESK
CAIRN
RIVER

"AS THE INITIAL BREAKS DEVELOPED INTO THRUSTS, NEW ONES FORMED AND EVENTUALLY THE VARIOUS EXTENSIONS OF THE THRUSTS INTERLOCKED, MERGED, OR SUBSIDIARY CONNECTING FAULTS FORMED BETWEEN THEM."

R.J.W. Douglas, 1958, Mount Head Map-Area, Alberta. Geological Survey of Canada Memoir 291, p.131.

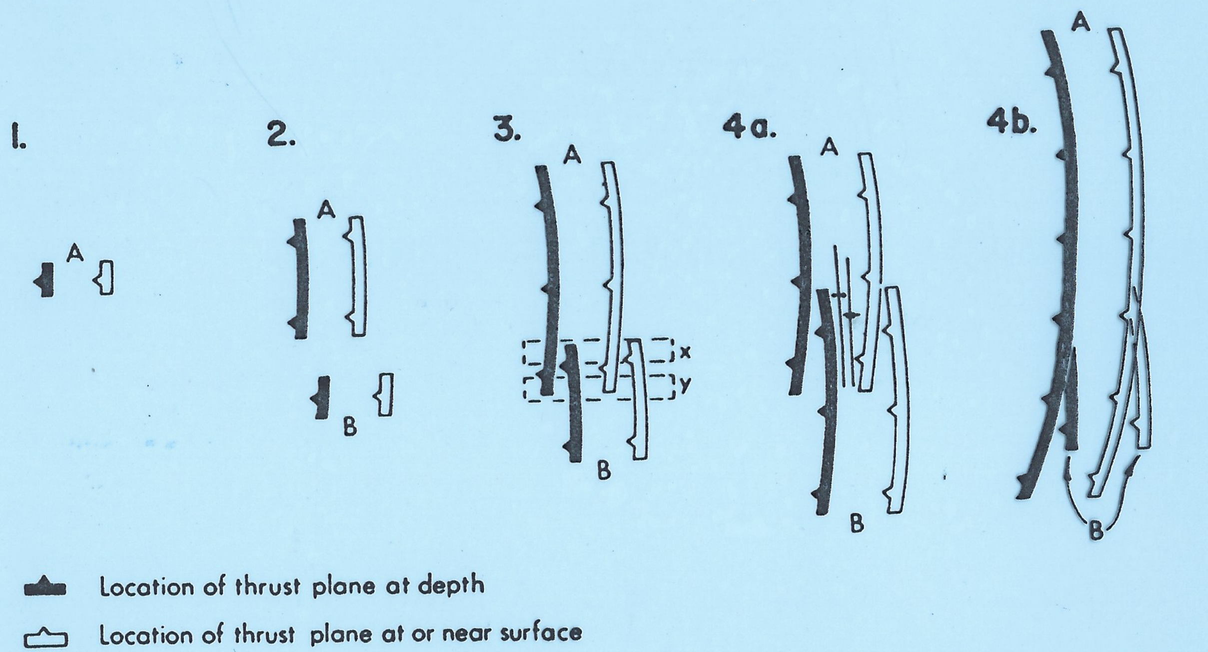

FIG. 10.—Diagram of show time and space relations between successive thrusts (plan view). **1.** Initial break of thrust A. **2.** Movement of A, initial break of thrust B. **3.** Movement of A and B. At X, thrust A is older than B. At Y, thrust A is younger than B. **4a.** Movement of thrust A ceases. Continued movement of B causes folding of thrust A. **4b.** Movement of B ceases. Continued movement of A causes it to override B.

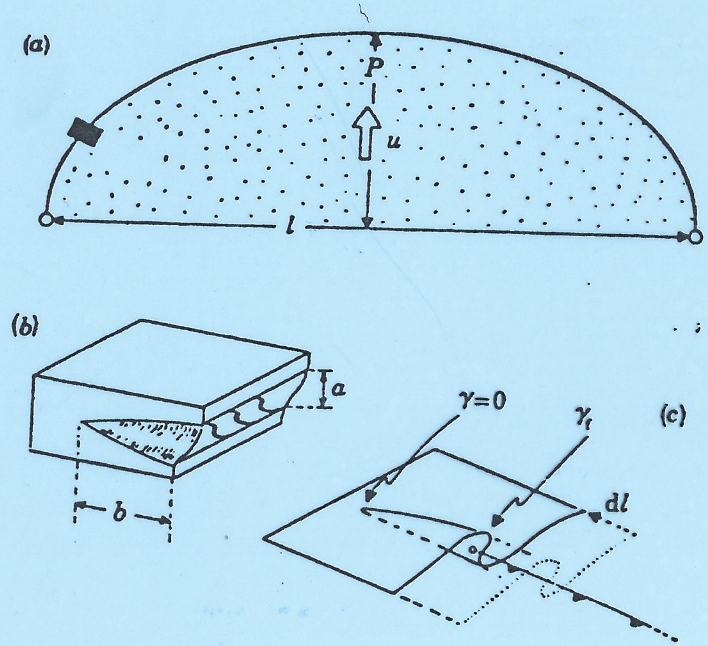

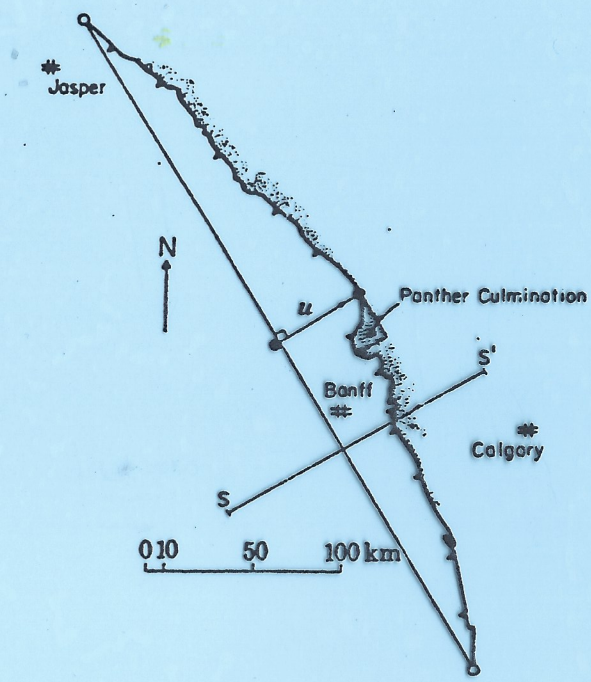

Elliot, D, 1976, The energy balance and deformation mechanisms of thrust sheets. Phil. Trans. R. Soc. London, A283: p 289-312.

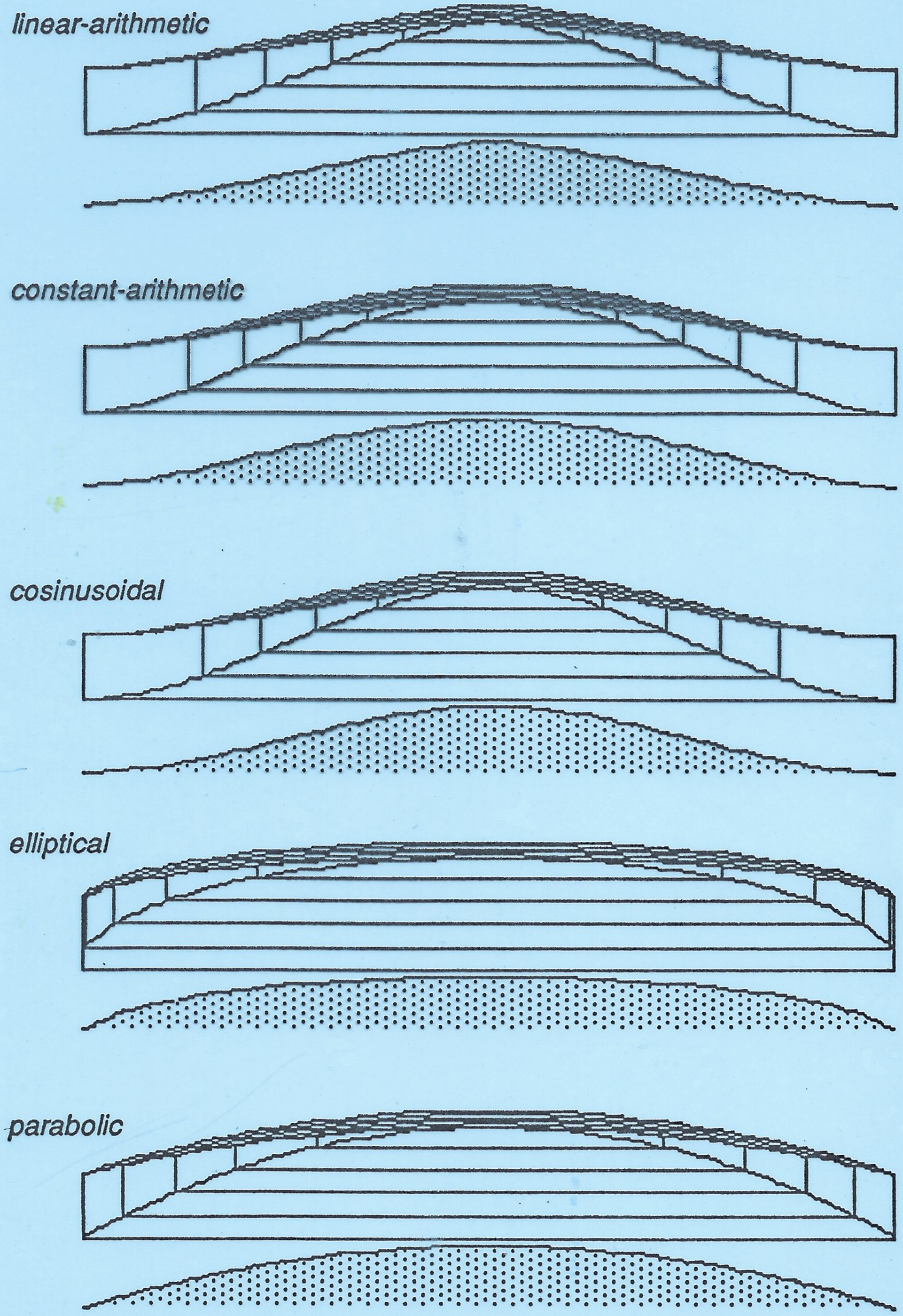

Figure 7(b). Contour maps and trailing-edge displacement profiles for 29°-ramp fault-propagation folds generated by various displacement functions. Fault parameters correspond to 5 km maximum displacement stage of Table 5. Contour interval 1 km.

Ratliff, R.A., 1994, Three-Dimensional Fault-Propagation Folding: a Model Based on Displacement Variation. Journal of Structural Geology.

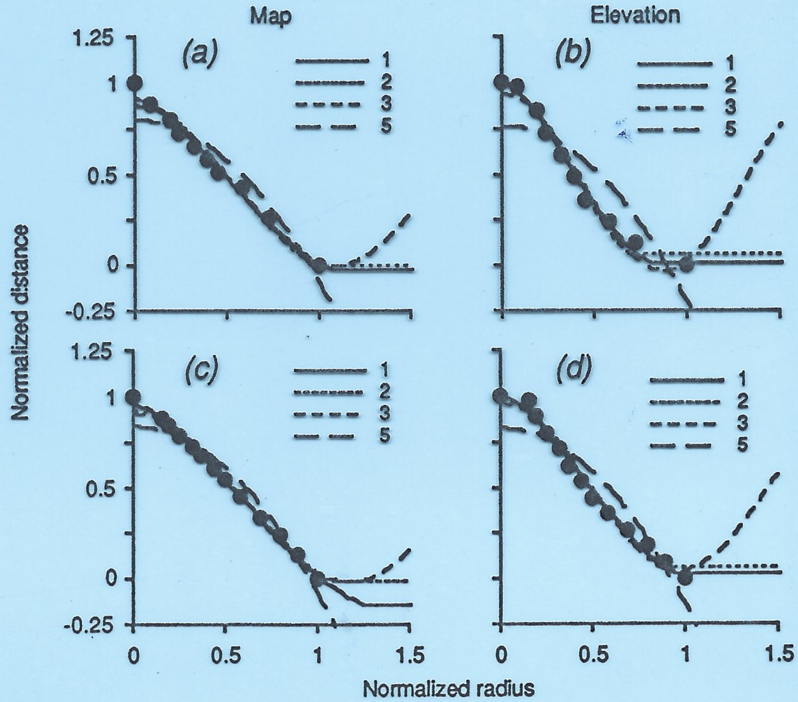

Figure 17. Map and elevation projections and best-fit analytic curve solutions for Frannie North (a) and (b) and Frannie South (c) and (d) hinge lines (see Fig. 15). Curves: 1, linear-arithmetic; 2, constant-arithmetic; 3, cosinusoidal; 5, parabolic. The linear-arithmetic curve is best-fitting solution for each projection, with no convergence for elliptical functions.

Table 6. Results of least-squares curve-fitting for different functions.

	Analytical curve	Mean ($^1\chi^2$)	Median ($^1\chi^2$)	Minimum ($^1\chi^2$)	Maximum ($^1\chi^2$)	^2n
Map projection	Linear-arithmetic	0.0272	0.0110	0.0000	0.3728	91
	Constant-arithmetic	0.0315	0.0119	0.0001	0.3867	115
	Cosinusoidal	0.0295	0.0130	0.0001	0.2308	117
	Elliptical	0.0513	0.0240	0.0002	0.6883	68
	Parabolic	0.1006	0.0561	0.0004	0.8616	195
Elevation projection	Linear-arithmetic	0.0088	0.0048	0.0000	0.0816	98
	Constant-arithmetic	0.0099	0.0062	0.0000	0.0912	124
	Cosinusoidal	0.2344	0.0061	0.0000	29.4626	132
	Elliptical	0.0149	0.0078	0.0000	0.0678	60
	Parabolic	0.2003	0.0298	0.0001	29.5084	195

[1] $\chi^2 = \sum_{i=1}^{n} (y_i - \hat{y}_i)^2$, y_i and $\hat{y}_i$ are the observed and predicted displacement values, respectively.

[2] Number of convergent least-squares solutions.

Ratliff, R.A., 1994, Three-Dimensional Fault-Propagation Folding: a Model Based on Displacement Variation. Journal of Structural Geology.

linear-arithmetic, $d = a + b\left[1 - \left(\frac{r}{c}\right)^{3/2}\right]\left[1 - \left(\frac{2r}{r+c}\right)^2\right]^{1/2}$; (12)

constant-arithmetic, $d = a + 2b\left(1 - \frac{r}{c}\right)\left[\left(\frac{1 + \frac{r}{c}}{2}\right)^2 - \left(\frac{r}{c}\right)^2\right]^{1/2}$; (13)

cosinusoidal, $d = a + \frac{b}{2}\left[1 + \cos\left(\frac{\pi r}{c}\right)\right]$; (14)

elliptical, $d = a + \left[b^2 - \left(\frac{b r}{c}\right)^2\right]^{1/2}$; (15)

and parabolic, $d = a + b\left[1 - \left(\frac{r}{c}\right)^2\right]$. (16)

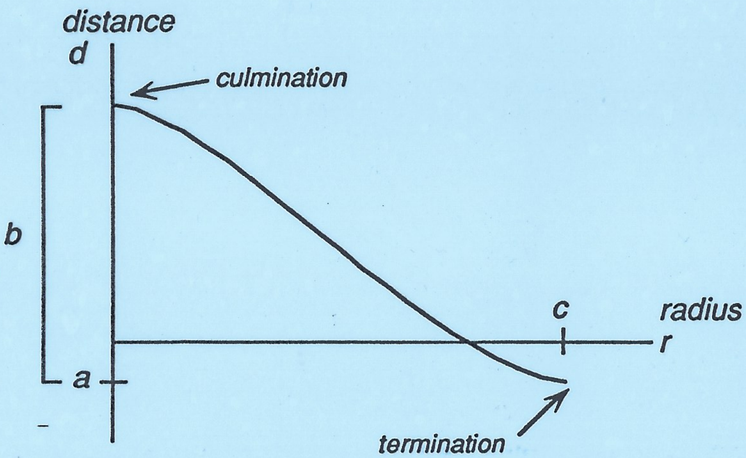

Figure 16. Parameter definitions for least-squares curve-fitting.

Ratliff, R.A., 1994, Three-Dimensional Fault-Propagation Folding: a Model Based on Displacement Variation. Journal of Structural Geology.

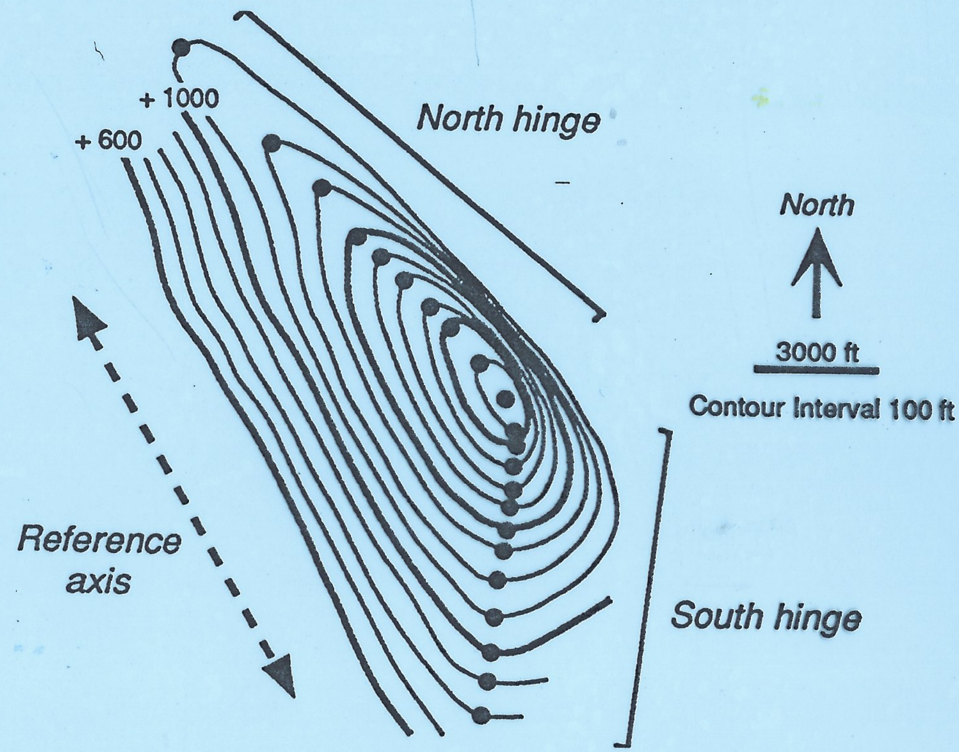

Figure 15. Loci of points defining north and south hinge lines of Frannie fold, Park County, Wyoming (WGA 1989). North hinge appears to represent boundary between forelimb and backlimb domains; south hinge corresponds to crest-backlimb boundary.

Ratliff, R.A., 1994, Three-Dimensional Fault-Propagation Folding: a Model Based on Displacement Variation. Journal of Structural Geology.

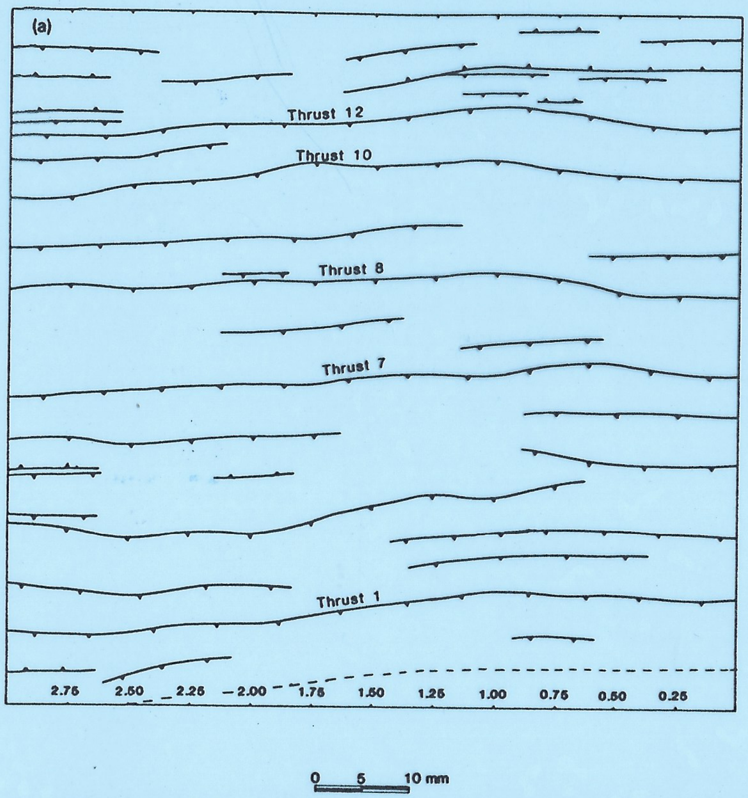

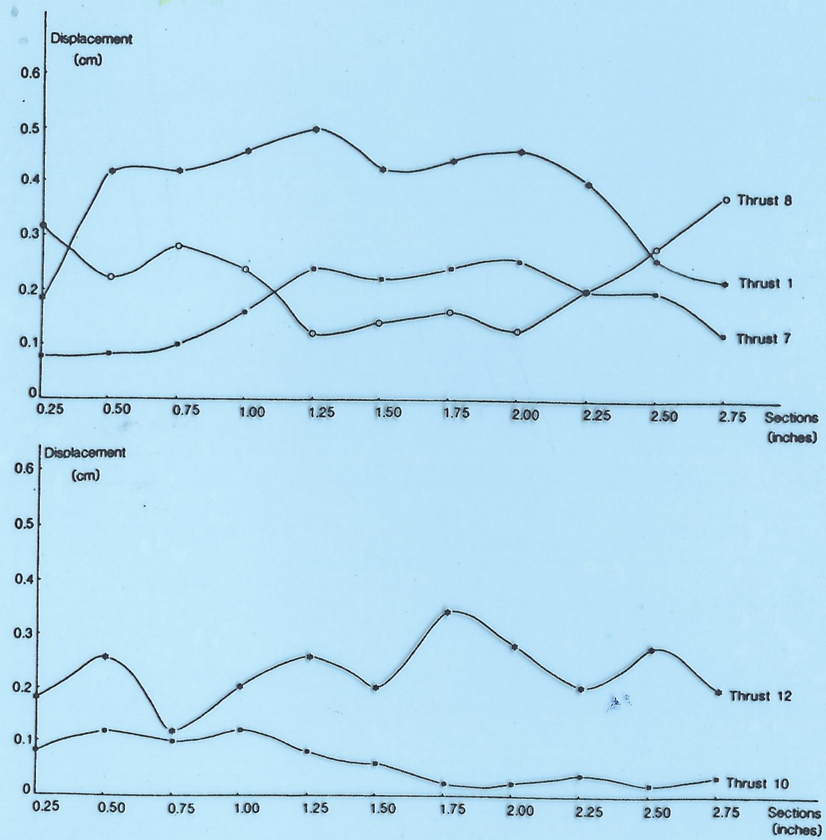

Fig. 11. Along-strike variation of thrust displacement for five thrusts in unit V, model TH-22.

Liu, S. and Dixon, J.M., 1991. Centrifuge modelling of thrust faulting: structural variation along strike in fold-thrust belts. *In*: P.R. Cobbold (Editor), Experimental and Numerical Modelling of Continental Deformation. Tectonophysics, 188: 39-62.

LATERAL FAULT CAPTURE

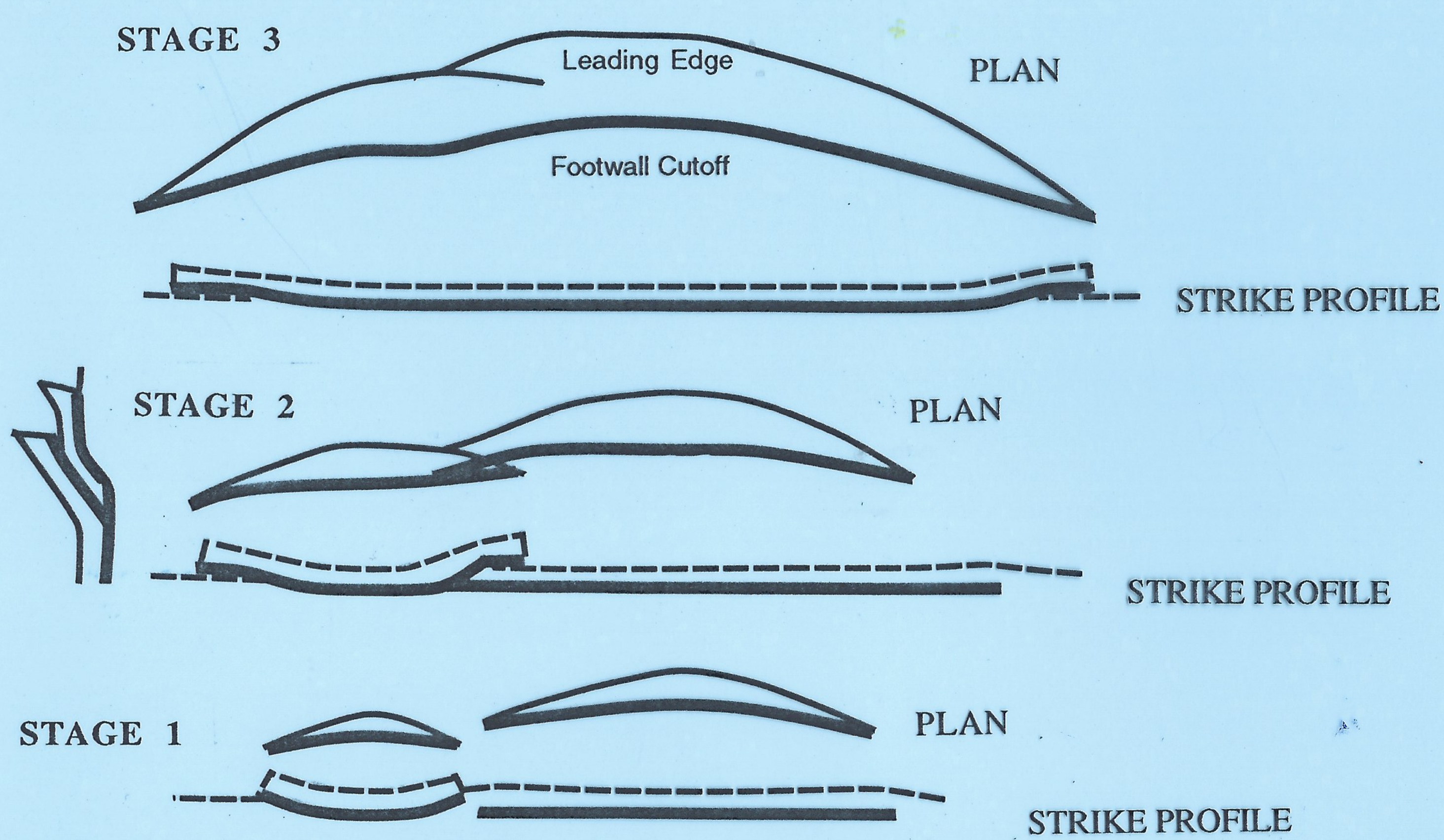

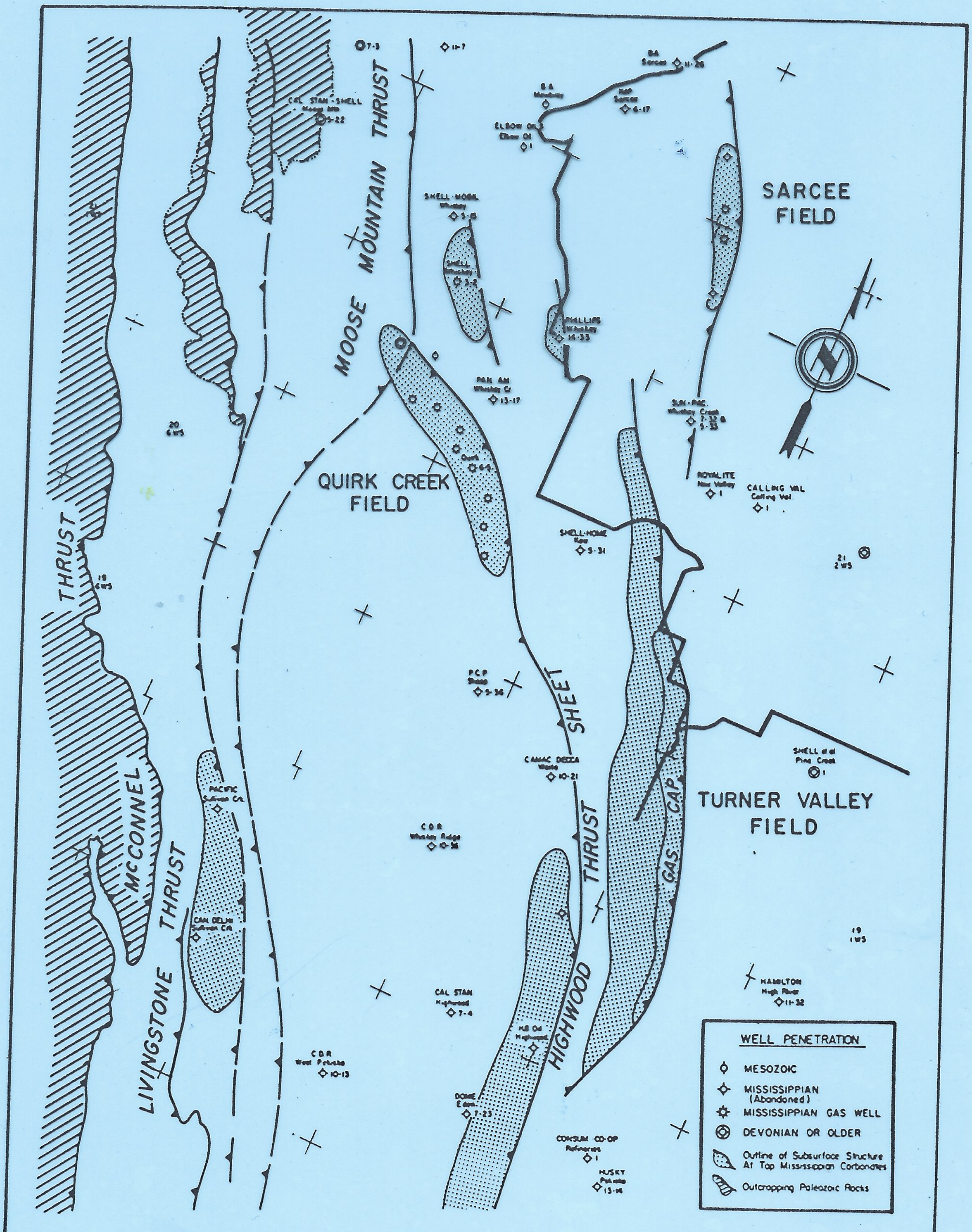

Figure 4 Well Location and Subsurface Structure Map I

QUIRK CREEK–HIGHWOOD THRUST RELATIONSHIP

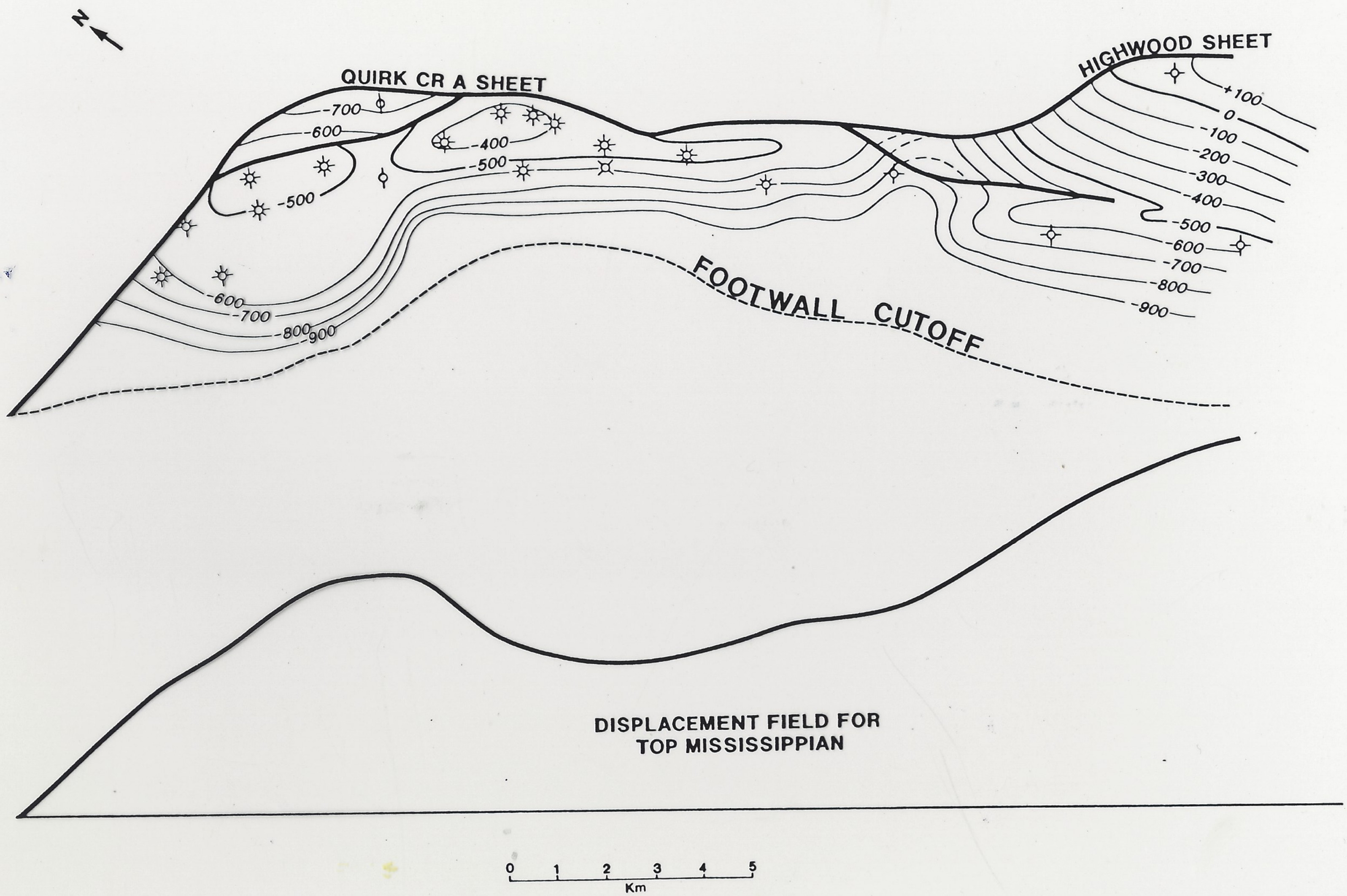

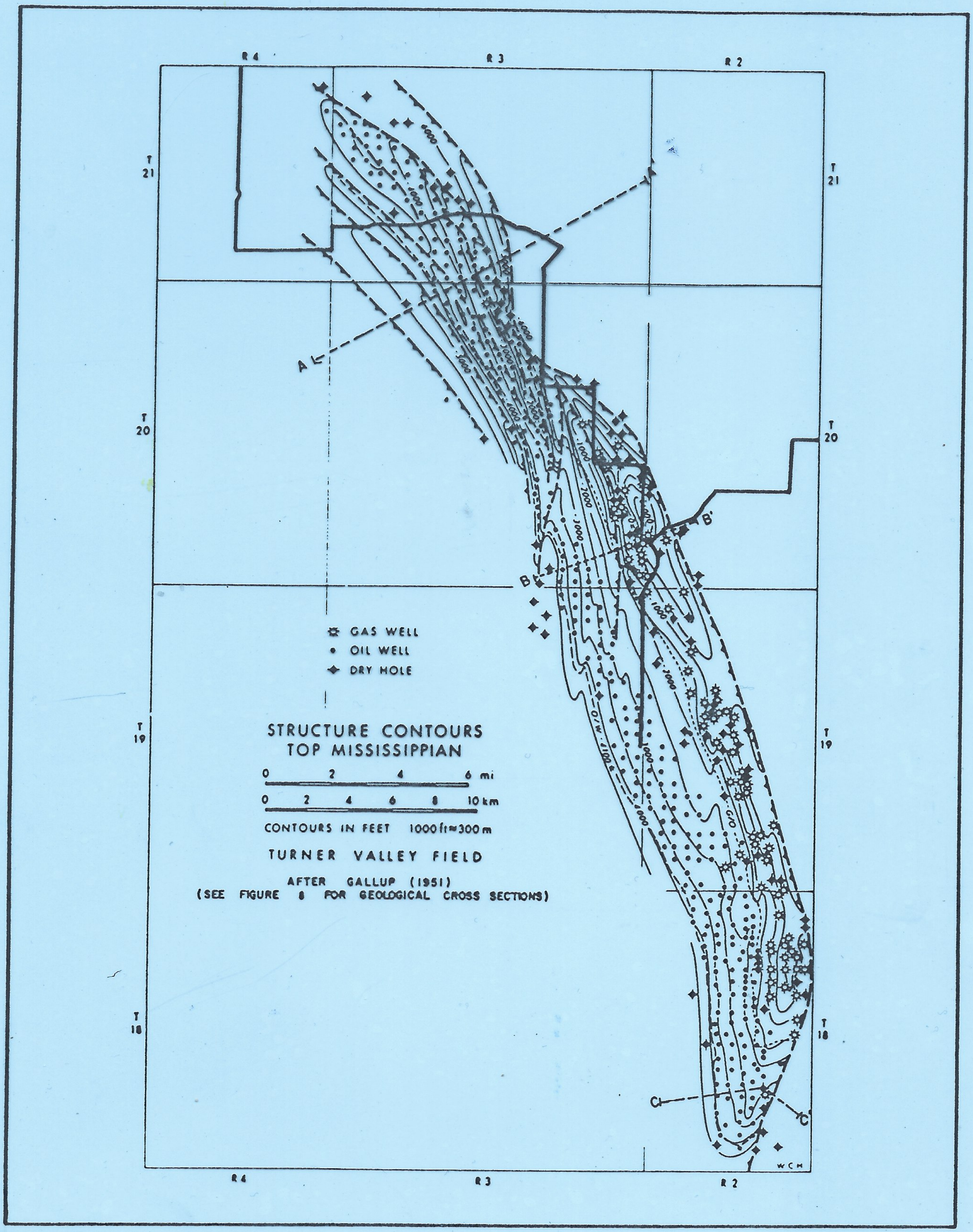

Figure 7 Structure Map Top Mississippian-Turner Valley Field (after Gallup 1951)

TOP MISSISSIPPIAN STRUCTURE CASTLE RIVER AREA

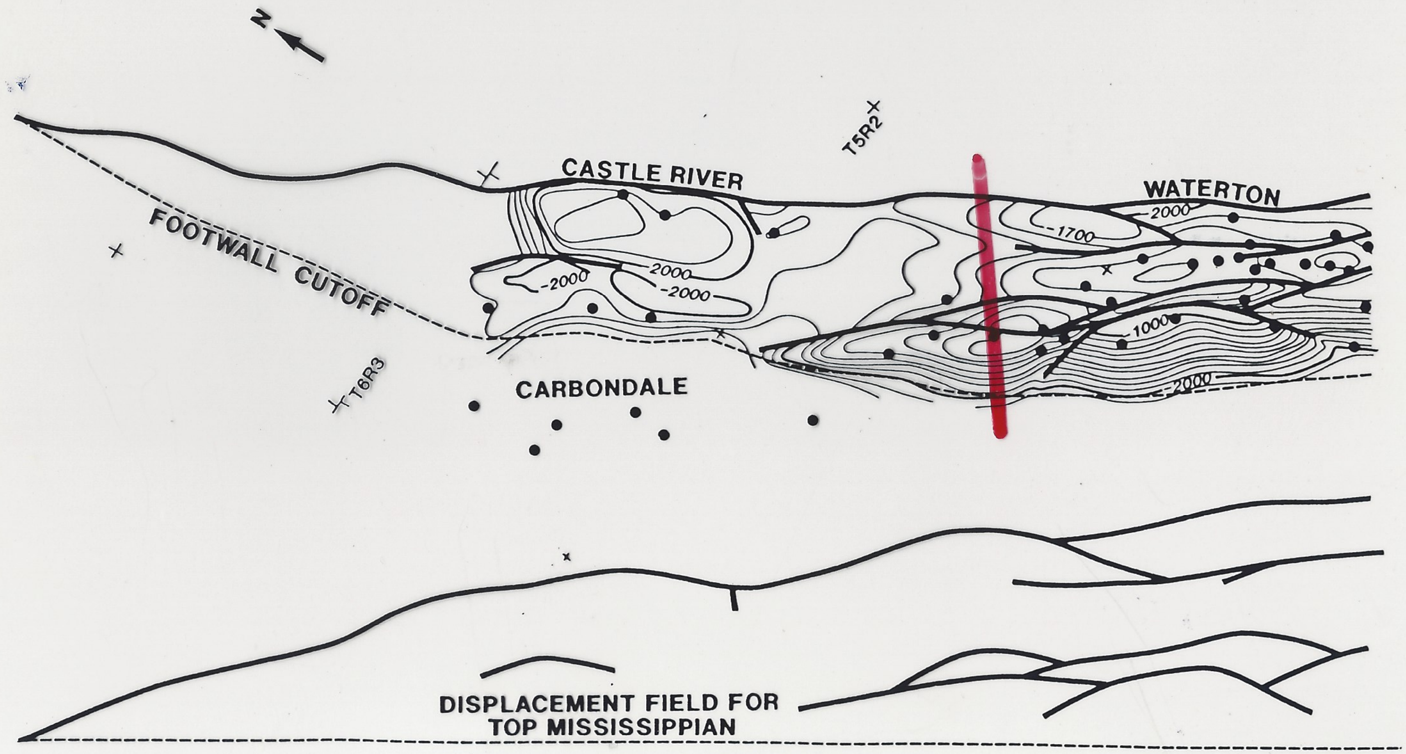

NORTH WATERTON SW ALBERTA
BALANCED STRUCTURE SECTION

Depth Interpretation 6J965

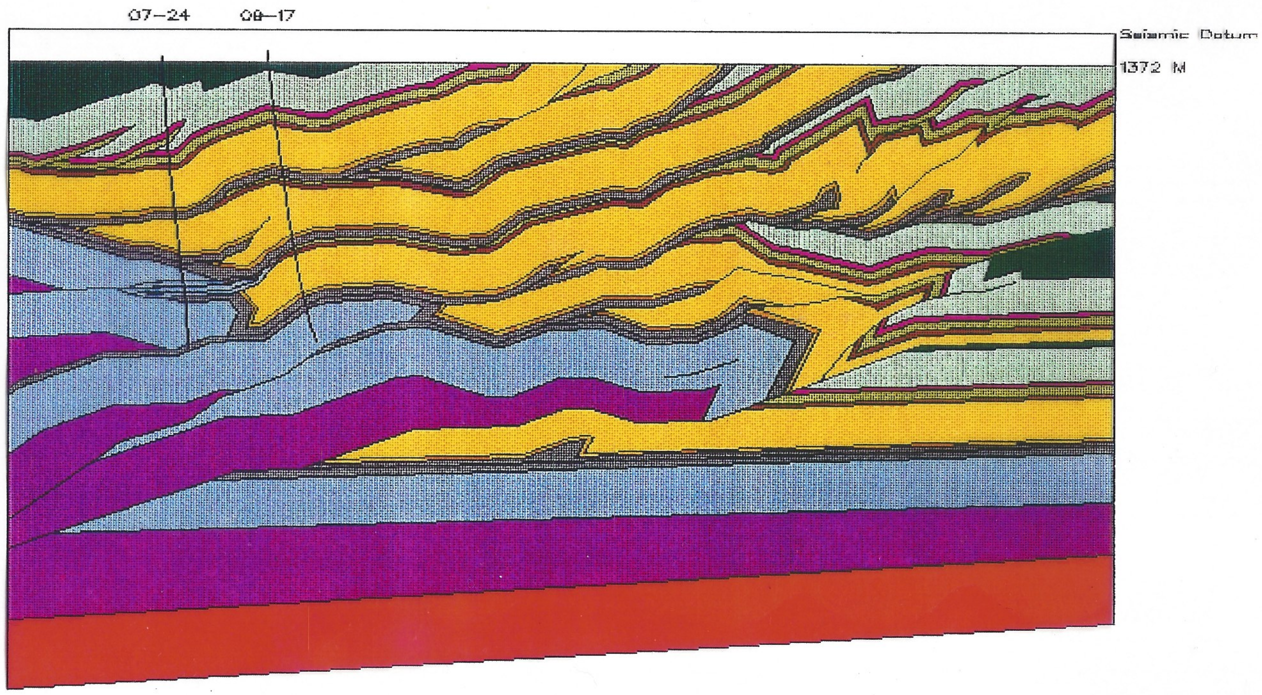

NORMAL LATERAL CAPTURE

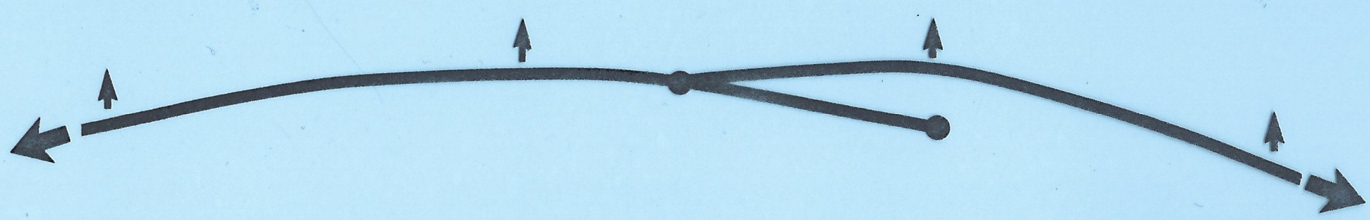

"OUT-OF-SEQUENCE" PROPAGATION

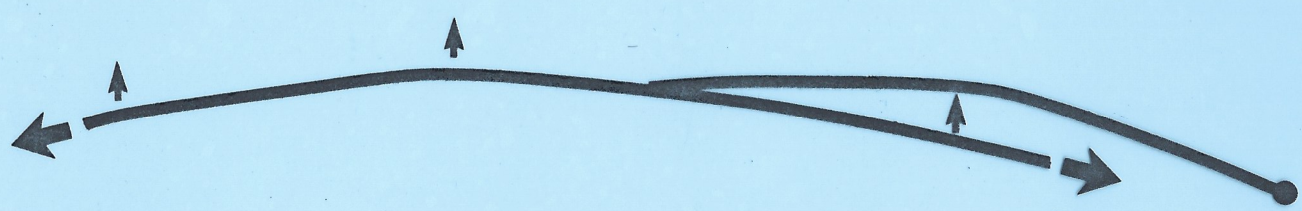

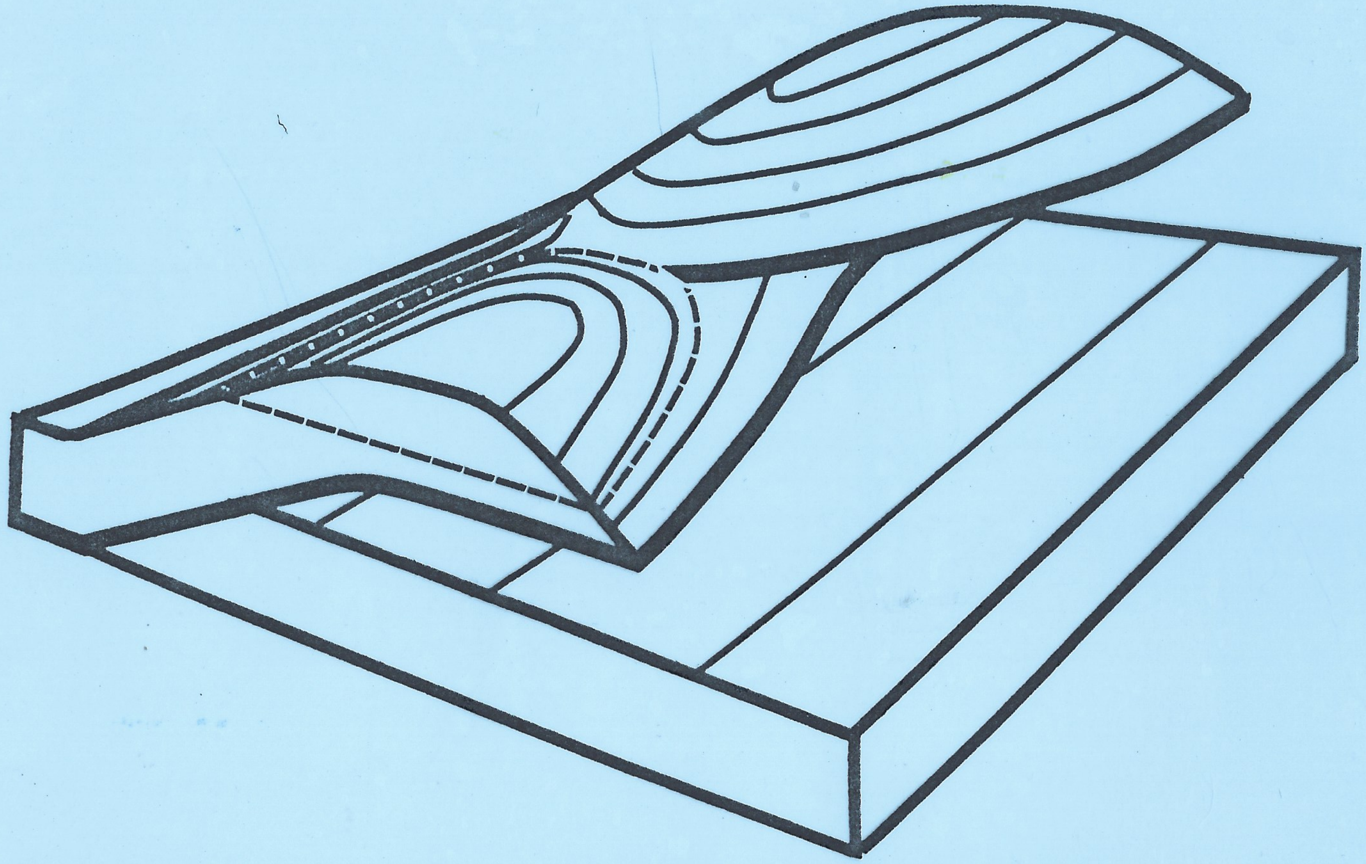

TRAP FILL LEVEL CONTROLLED BY LEAK POINT
ALONG FAULT NETWORK

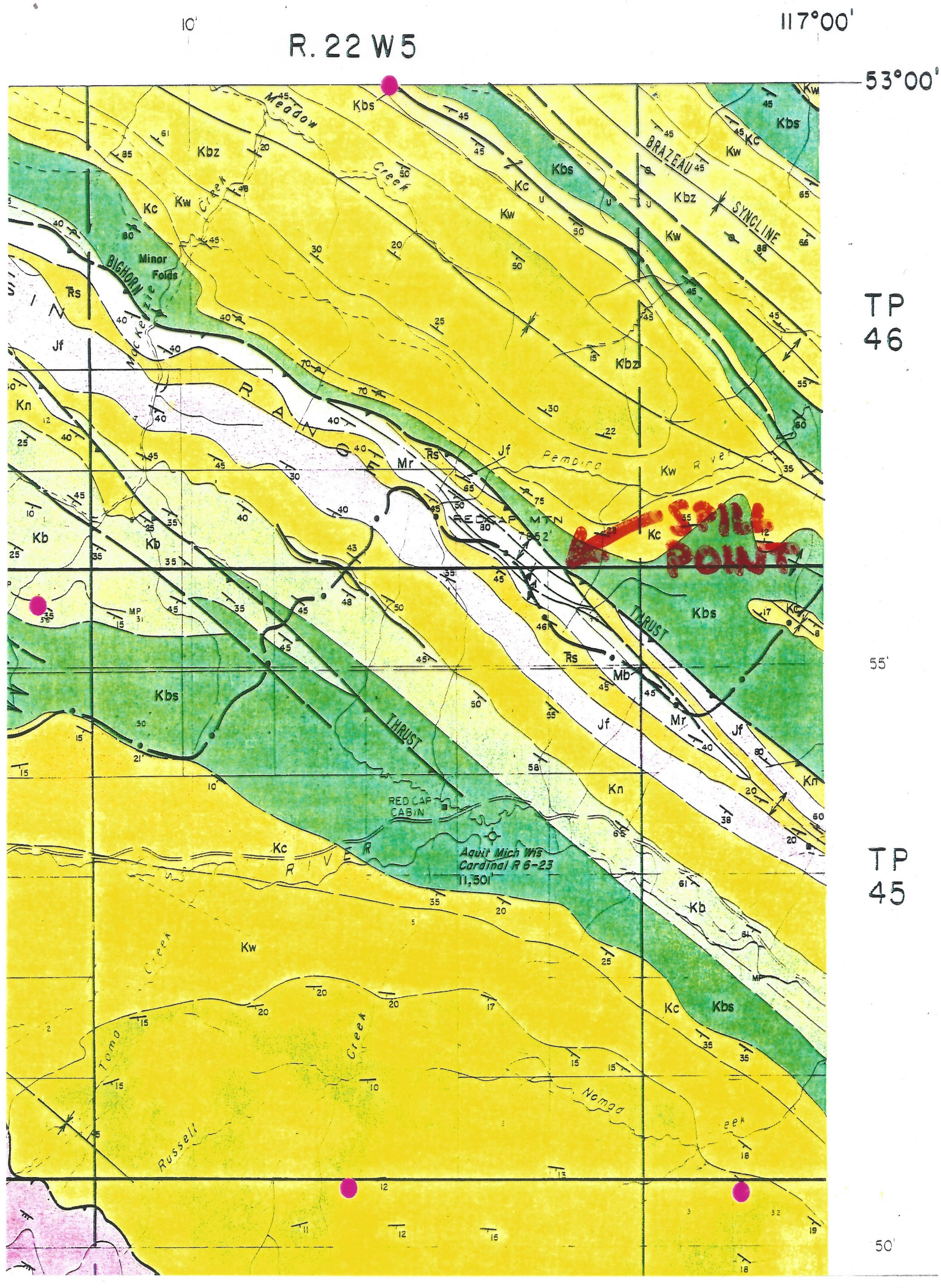
10'
R. 22 W5
117°00'
53°00'
TP 46
55'
TP 45
50'
Meadow Creek
BRAZEAU SYNCLINE
BIGHORN
Minor Folds
RANGE
Pembina River
REDCAP MTN 7852'
SPILL POINT
THRUST
RED CAP CABIN
Aquit Mich Wis Cardinal R 6-23 11,501'
RIVER
Tomo Creek
Russell
Nomga Creek
Kbs
Kbz
Kc
Kw
Rs
Jf
Kn
Kb
Mr
Mb
MP

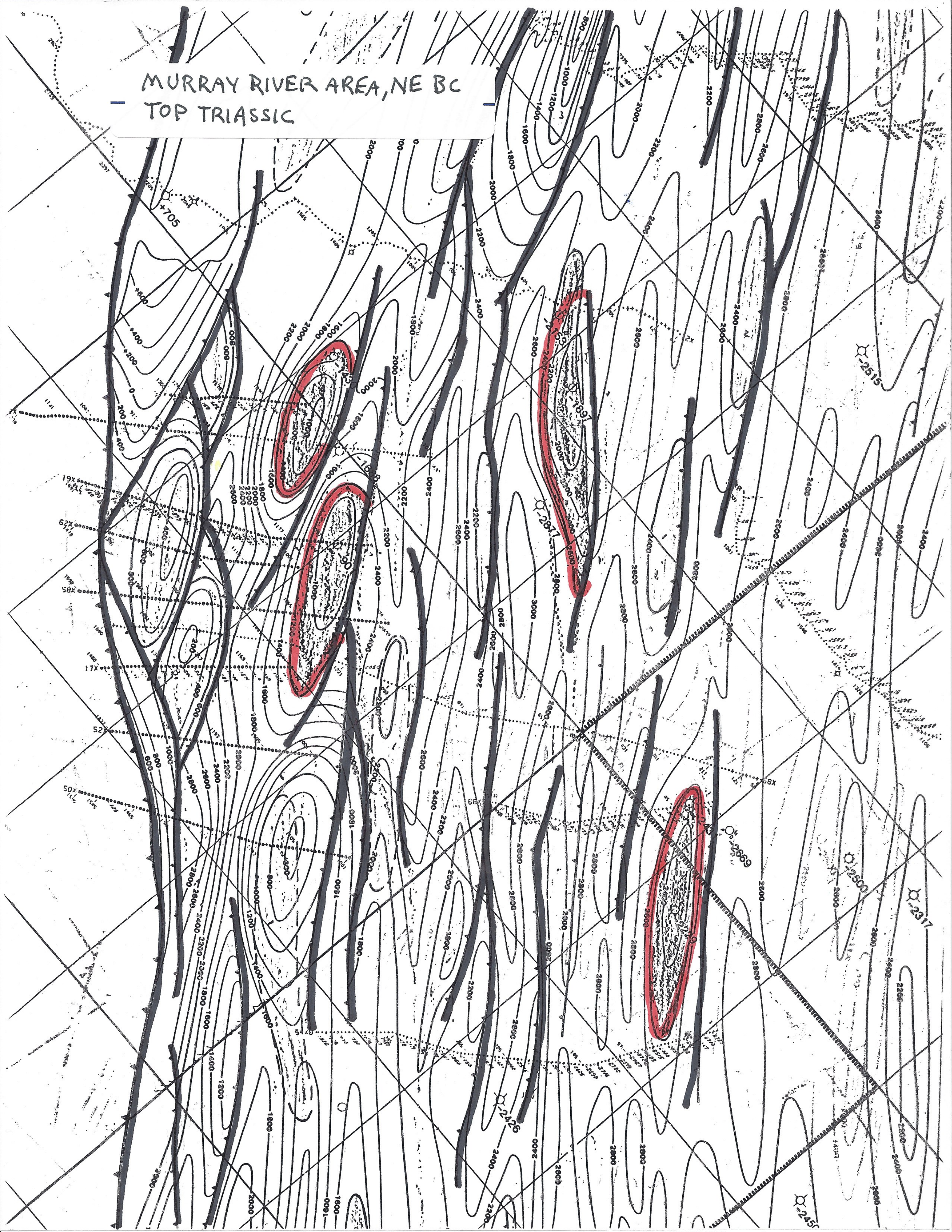
MURRAY RIVER AREA, NE BC
TOP TRIASSIC
+705
-2515
-2669
-2500
-2317
-2426